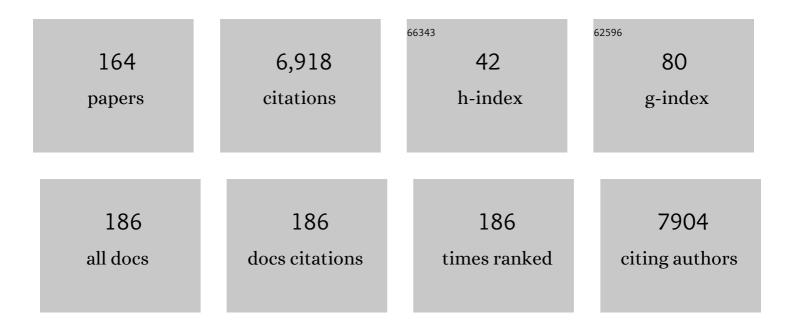
Sandra Van Aert

List of Publications by Year in descending order

Source: https://exaly.com/author-pdf/2204854/publications.pdf Version: 2024-02-01



SANDDA VAN AFDT

#	Article	IF	CITATIONS
1	Dynamical diffraction of high-energy electrons investigated by focal series momentum-resolved scanning transmission electron microscopy at atomic resolution. Ultramicroscopy, 2022, 233, 113425.	1.9	5
2	Atomic resolution electron tomography: a dream?. International Journal of Materials Research, 2022, 97, 872-879.	0.3	0
3	From 2D to 3D: Bridging Self-Assembled Monolayers to a Substrate-Induced Polymorph in a Molecular Semiconductor. Chemistry of Materials, 2022, 34, 2238-2248.	6.7	11
4	Monitoring oxygen production on mass-selected iridium–tantalum oxide electrocatalysts. Nature Energy, 2022, 7, 55-64.	39.5	108
5	Atomic-scale detection of individual lead clusters confined in Linde Type A zeolites. Nanoscale, 2022, 14, 9323-9330.	5.6	2
6	Thermal Activation of Gold Atom Diffusion in Au@Pt Nanorods. ACS Nano, 2022, 16, 9608-9619.	14.6	8
7	Efficient fitting algorithm. Advances in Imaging and Electron Physics, 2021, 217, 73-90.	0.2	0
8	Atom column detection. Advances in Imaging and Electron Physics, 2021, 217, 177-214.	0.2	3
9	Atom counting. Advances in Imaging and Electron Physics, 2021, , 91-144.	0.2	1
10	Statistical parameter estimation theory: principles and simulation studies. Advances in Imaging and Electron Physics, 2021, , 29-72.	0.2	2
11	Optimal experiment design for nanoparticle atom counting from ADF STEM images. Advances in Imaging and Electron Physics, 2021, 217, 145-175.	0.2	0
12	Three-dimensional atomic structure of supported Au nanoparticles at high temperature. Nanoscale, 2021, 13, 1770-1776.	5.6	13
13	General conclusions and future perspectives. Advances in Imaging and Electron Physics, 2021, , 243-253.	0.2	0
14	Image-quality evaluation and model selection with maximum a posteriori probability. Advances in Imaging and Electron Physics, 2021, 217, 215-242.	0.2	0
15	Three-Dimensional Nanoparticle Transformations Captured by an Electron Microscope. Accounts of Chemical Research, 2021, 54, 1189-1199.	15.6	13
16	3D Atomicâ€Scale Dynamics of Laserâ€Lightâ€Induced Restructuring of Nanoparticles Unraveled by Electron Tomography. Advanced Materials, 2021, 33, 2100972.	21.0	10
17	Combining ADF-EDX scattering cross-sections for elemental quantification of nanostructures. Microscopy and Microanalysis, 2021, 27, 600-602.	0.4	1
18	Phase Retrieval From 4-Dimensional Electron Diffraction Datasets. , 2021, , .		0

#	Article	IF	CITATIONS
19	Coupling Charge and Topological Reconstructions at Polar Oxide Interfaces. Physical Review Letters, 2021, 127, 127202.	7.8	20
20	Modelling ADF STEM images using elliptical Gaussian peaks and its effects on the quantification of structure parameters in the presence of sample tilt. Ultramicroscopy, 2021, 230, 113391.	1.9	3
21	Interface Pattern Engineering in Coreâ€Shell Upconverting Nanocrystals: Shedding Light on Critical Parameters and Consequences for the Photoluminescence Properties. Small, 2021, 17, e2104441.	10.0	17
22	3D Atomic Structure of Supported Metallic Nanoparticles Estimated from 2D ADF STEM Images: A Combination of Atom ounting and a Local Minima Search Algorithm. Small Methods, 2021, 5, e2101150.	8.6	10
23	Interface Pattern Engineering in Coreâ€Shell Upconverting Nanocrystals: Shedding Light on Critical Parameters and Consequences for the Photoluminescence Properties (Small 47/2021). Small, 2021, 17, 2170246.	10.0	0
24	Hidden Markov model for atom-counting from sequential ADF STEM images: Methodology, possibilities and limitations. Ultramicroscopy, 2020, 219, 113131.	1.9	2
25	Alloy CsCd <i>_x</i> Pb _{1–<i>x</i>} Br ₃ Perovskite Nanocrystals: The Role of Surface Passivation in Preserving Composition and Blue Emission. Chemistry of Materials, 2020, 32, 10641-10652.	6.7	45
26	3D Characterization and Plasmon Mapping of Gold Nanorods Welded by Femtosecond Laser Irradiation. ACS Nano, 2020, 14, 12558-12570.	14.6	30
27	Novel Approaches for Electron Tomography to Investigate the Structure and Stability of Nanomaterials in 3 Dimensions Microscopy and Microanalysis, 2020, 26, 1128-1130.	0.4	1
28	3D Atomic Scale Quantification of Nanostructures and their Dynamics Using Model-based STEM. Microscopy and Microanalysis, 2020, 26, 2606-2608.	0.4	1
29	Atom column detection from simultaneously acquired ABF and ADF STEM images. Ultramicroscopy, 2020, 219, 113046.	1.9	15
30	Measuring Dynamic Structural Changes of Nanoparticles at the Atomic Scale Using Scanning Transmission Electron Microscopy. Physical Review Letters, 2020, 124, 106105.	7.8	20
31	Berry phase engineering at oxide interfaces. Physical Review Research, 2020, 2, .	3.6	64
32	Quantification of 3D Atomic Structures and Their Dynamics by Atom-Counting from an ADF STEM Image. Microscopy and Microanalysis, 2019, 25, 1808-1809.	0.4	0
33	Selfâ€Assembly of Atomically Thin Chiral Copper Heterostructures Templated by Black Phosphorus. Advanced Functional Materials, 2019, 29, 1903120.	14.9	9
34	Quantitative 3D Characterization of Elemental Diffusion Dynamics in Individual Ag@Au Nanoparticles with Different Shapes. ACS Nano, 2019, 13, 13421-13429.	14.6	37
35	Electrical Polarization in AlN/GaN Nanodisks Measured by Momentum-Resolved 4D Scanning Transmission Electron Microscopy. Physical Review Letters, 2019, 122, 106102.	7.8	31
36	The maximum a posteriori probability rule for atom column detection from HAADF STEM images. Ultramicroscopy, 2019, 201, 81-91.	1.9	17

#	Article	IF	CITATIONS
37	The atomic lensing model: New opportunities for atom-by-atom metrology of heterogeneous nanomaterials. Ultramicroscopy, 2019, 203, 155-162.	1.9	12
38	Control of Knock-On Damage for 3D Atomic Scale Quantification of Nanostructures: Making Every Electron Count in Scanning Transmission Electron Microscopy. Physical Review Letters, 2019, 122, 066101.	7.8	14
39	Comparison of first moment STEM with conventional differential phase contrast and the dependence on electron dose. Ultramicroscopy, 2019, 203, 95-104.	1.9	29
40	Three-Dimensional Quantification of the Facet Evolution of Pt Nanoparticles in a Variable Gaseous Environment. Nano Letters, 2019, 19, 477-481.	9.1	93
41	Model-Based Electron Microscopy. Springer Handbooks, 2019, , 605-624.	0.6	2
42	Thickness dependence of scattering cross-sections in quantitative scanning transmission electron microscopy. Ultramicroscopy, 2018, 187, 84-92.	1.9	11
43	Frozen lattice and absorptive model for high angle annular dark field scanning transmission electron microscopy: A comparison study in terms of integrated intensity and atomic column position measurement. Ultramicroscopy, 2018, 184, 188-198.	1.9	4
44	Atomic-scale quantification of charge densities in two-dimensional materials. Physical Review B, 2018, 98, .	3.2	36
45	Metal–insulator-transition engineering by modulation tilt-control in perovskite nickelates for room temperature optical switching. Proceedings of the National Academy of Sciences of the United States of America, 2018, 115, 9515-9520.	7.1	56
46	Single Atom Detection from Low Contrast-to-Noise Ratio Electron Microscopy Images. Physical Review Letters, 2018, 121, 056101.	7.8	30
47	Recent Advances in Transmission Electron Microscopy for Materials Science at the EMAT Lab of the University of Antwerp. Materials, 2018, 11, 1304.	2.9	19
48	Recent breakthroughs in scanning transmission electron microscopy of small species. Advances in Physics: X, 2018, 3, 1480420.	4.1	11
49	Understanding the Effect of Iodide Ions on the Morphology of Gold Nanorods. Particle and Particle Systems Characterization, 2018, 35, 1800051.	2.3	6
50	Present state of the composition evaluation of ternary semiconductor nanostructures by lattice fringe analysis. , 2018, , 19-22.		0
51	How precise can atoms of a nanocluster be located in 3D using a tilt series of scanning transmission electron microscopy images?. Ultramicroscopy, 2017, 181, 134-143.	1.9	6
52	Quantification by aberration corrected (S)TEM of boundaries formed by symmetry breaking phase transformations. Ultramicroscopy, 2017, 176, 194-199.	1.9	2
53	Controlled growth of hexagonal gold nanostructures during thermally induced self-assembling on Ge(001) surface. Scientific Reports, 2017, 7, 42420.	3.3	28
54	Highly Emissive Divalent-Ion-Doped Colloidal CsPb _{1–<i>x</i>} M _{<i>x</i>} Br ₃ Perovskite Nanocrystals through Cation Exchange. Journal of the American Chemical Society, 2017, 139, 4087-4097.	13.7	590

#	Article	IF	CITATIONS
55	Three-dimensional atomic models from a single projection using Z-contrast imaging: verification by electron tomography and opportunities. Nanoscale, 2017, 9, 8791-8798.	5.6	44
56	One Step Toward a New Generation of C-MOS Compatible Oxide P–N Junctions: Structure of the LSMO/ZnO Interface Elucidated by an Experimental and Theoretical Synergic Work. ACS Applied Materials & Interfaces, 2017, 9, 20974-20980.	8.0	4
57	Hybrid statistics-simulations based method for atom-counting from ADF STEM images. Ultramicroscopy, 2017, 177, 69-77.	1.9	30
58	Ligand-Induced Shape Transformation of PbSe Nanocrystals. Chemistry of Materials, 2017, 29, 4122-4128.	6.7	45
59	Thickness Dependent Properties in Oxide Heterostructures Driven by Structurally Induced Metal–Oxygen Hybridization Variations. Advanced Functional Materials, 2017, 27, 1606717.	14.9	61
60	Recent Advances of the Open Source MULTEM Program to Provide Accurate and Fast Electron Microscopy Simulations. Microscopy and Microanalysis, 2017, 23, 206-207.	0.4	0
61	Quantitative STEM of Catalyst Nanoparticles using ADF Imaging with Simultaneous EDS and EELS Spectroscopy Microscopy and Microanalysis, 2017, 23, 1888-1889.	0.4	0
62	Atom-counting in High Resolution Electron Microscopy:TEM or STEM – That's the question. Ultramicroscopy, 2017, 174, 112-120.	1.9	7
63	Depth sectioning combined with atom-counting in HAADF STEM to retrieve the 3D atomic structure. Ultramicroscopy, 2017, 177, 36-42.	1.9	13
64	Locating light and heavy atomic column positions with picometer precision using ISTEM. Ultramicroscopy, 2017, 172, 75-81.	1.9	9
65	StatSTEM: An efficient program for accurate and precise model-based quantification of atomic resolution electron microscopy images. Journal of Physics: Conference Series, 2017, 902, 012013.	0.4	4
66	Determining oxygen relaxations at an interface: A comparative study between transmission electron microscopy techniques. Ultramicroscopy, 2017, 181, 178-190.	1.9	36
67	Atomic resolution electron tomography. MRS Bulletin, 2016, 41, 525-530.	3.5	24
68	Quantifying a Heterogeneous Ru Catalyst on Carbon Black Using ADF STEM. Particle and Particle Systems Characterization, 2016, 33, 438-444.	2.3	9
69	Quantification of ADF STEM Image Data for Nanoparticle Structure and Strain Measurements. Microscopy and Microanalysis, 2016, 22, 896-897.	0.4	0
70	Advanced electron crystallography through model-based imaging. IUCrJ, 2016, 3, 71-83.	2.2	36
71	In situ study of the formation mechanism ofÂtwo-dimensional superlattices from PbSeÂnanocrystals. Nature Materials, 2016, 15, 1248-1254.	27.5	199
72	Detecting and locating light atoms from high-resolution STEM images: The quest for a single optimal design. Ultramicroscopy, 2016, 170, 128-138.	1.9	11

#	Article	IF	CITATIONS
73	StatSTEM: An efficient approach for accurate and precise model-based quantification of atomic resolution electron microscopy images. Ultramicroscopy, 2016, 171, 104-116.	1.9	170
74	Direct Methods for Images Interpretation. , 2016, , 267-281.		0
75	Direct Observation of Ferroelectric Domain Walls in LiNbO ₃ : Wallâ€Meanders, Kinks, and Local Electric Charges. Advanced Functional Materials, 2016, 26, 7599-7604.	14.9	72
76	Unscrambling Mixed Elements using High Angle Annular Dark Field Scanning Transmission Electron Microscopy. Physical Review Letters, 2016, 116, 246101.	7.8	45
77	Longâ€Range Domain Structure and Symmetry Engineering by Interfacial Oxygen Octahedral Coupling at Heterostructure Interface. Advanced Functional Materials, 2016, 26, 6627-6634.	14.9	25
78	Progress and new advances in simulating electron microscopy datasets using MULTEM. Ultramicroscopy, 2016, 168, 17-27.	1.9	51
79	Controlled lateral anisotropy in correlated manganite heterostructures by interface-engineered oxygen octahedral coupling. Nature Materials, 2016, 15, 425-431.	27.5	292
80	Materials Science Applications of Aberration Corrected TEM and/or STEM. Microscopy and Microanalysis, 2015, 21, 1131-1132.	0.4	0
81	Quantitative annular dark field scanning transmission electron microscopy for nanoparticle atom-counting: What are the limits?. Journal of Physics: Conference Series, 2015, 644, 012034.	0.4	0
82	Quantitative STEM normalisation: The importance of the electron flux. Ultramicroscopy, 2015, 159, 46-58.	1.9	26
83	Determination of the atomic width of an APB in ordered CoPt using quantified HAADF-STEM. Journal of Alloys and Compounds, 2015, 644, 570-574.	5.5	15
84	Dose limited reliability of quantitative annular dark field scanning transmission electron microscopy for nano-particle atom-counting. Ultramicroscopy, 2015, 151, 56-61.	1.9	47
85	Optimal experimental design for nano-particle atom-counting from high-resolution STEM images. Ultramicroscopy, 2015, 151, 46-55.	1.9	42
86	Atomic and electronic structures of BaHfO ₃ -doped TFA-MOD-derived YBa ₂ Cu ₃ O _{7â~'<i>Î</i>} thin films. Superconductor Science and Technology, 2015, 28, 115009.	3.5	10
87	Smart Align—a new tool for robust non-rigid registration of scanning microscope data. Advanced Structural and Chemical Imaging, 2015, 1, .	4.0	290
88	Measuring Lattice Strain in Three Dimensions through Electron Microscopy. Nano Letters, 2015, 15, 6996-7001.	9.1	110
89	Optimal experimental design for the detection of light atoms from high-resolution scanning transmission electron microscopy images. Applied Physics Letters, 2014, 105, .	3.3	24
90	Lattice deformations in quasiâ€dynamic strain glass visualised and quantified by aberration corrected electron microscopy. Physica Status Solidi (B): Basic Research, 2014, 251, 2034-2040.	1.5	2

#	Article	IF	CITATIONS
91	The effect of probe inaccuracies on the quantitative model-based analysis of high angle annular dark field scanning transmission electron microscopy images. Micron, 2014, 63, 57-63.	2.2	26
92	A memory efficient method for fully three-dimensional object reconstruction with HAADF STEM. Ultramicroscopy, 2014, 141, 22-31.	1.9	9
93	Site occupation of Nb atoms in ternary Ni–Ti–Nb shape memory alloys. Acta Materialia, 2014, 74, 85-95.	7.9	36
94	Seeing and measuring in 3D with electrons. Comptes Rendus Physique, 2014, 15, 140-150.	0.9	17
95	Atomic Structure of Quantum Gold Nanowires: Quantification of the Lattice Strain. ACS Nano, 2014, 8, 599-606.	14.6	26
96	Quantitative composition determination at the atomic level using model-based high-angle annular dark field scanning transmission electron microscopy. Ultramicroscopy, 2014, 137, 12-19.	1.9	82
97	Atomic resolution mapping of phonon excitations in STEM-EELS experiments. Ultramicroscopy, 2014, 147, 1-7.	1.9	25
98	Getting the Best from an Imperfect Detector - an Alternative Normalisation Procedure for Quantitative HAADF STEM. Microscopy and Microanalysis, 2014, 20, 126-127.	0.4	1
99	An alternative approach to determine attainable resolution directly from HREM images. Ultramicroscopy, 2013, 133, 50-61.	1.9	2
100	Three-Dimensional Elemental Mapping at the Atomic Scale in Bimetallic Nanocrystals. Nano Letters, 2013, 13, 4236-4241.	9.1	101
101	Incommensurate Modulation and Luminescence in the CaGd _{2(l–<i>x</i>)} Eu _{2<i>x</i>/i>} (MoO ₄) _{4(l–<i>y</i>)} (W (0 ≤i>x ≤/i> 1, 0 ≤i>y ≤/i> 1) Red Phosphors. Chemistry of Materials, 2013, 25, 4387-4395.	/O e.s ub>4	<b gob>) <sub< td=""></sub<>
102	High resolution electron tomography. Current Opinion in Solid State and Materials Science, 2013, 17, 107-114.	11.5	31
103	Dedicated TEM on domain boundaries from phase transformations and crystal growth. Phase Transitions, 2013, 86, 15-22.	1.3	1
104	Atom counting in HAADF STEM using a statistical model-based approach: Methodology, possibilities, and inherent limitations. Ultramicroscopy, 2013, 134, 23-33.	1.9	95
105	Estimation of unknown structure parameters from high-resolution (S)TEM images: What are the limits?. Ultramicroscopy, 2013, 134, 34-43.	1.9	49
106	Functional twin boundaries. Phase Transitions, 2013, 86, 1052-1059.	1.3	7
107	Advanced three-dimensional electron microscopy techniques in the quest for better structural and functional materials. Science and Technology of Advanced Materials, 2013, 14, 014206.	6.1	14
108	Defect Engineering in Oxide Heterostructures by Enhanced Oxygen Surface Exchange. Advanced Functional Materials, 2013, 23, 5240-5248.	14.9	88

#	Article	lF	CITATIONS
109	Nano- and Microcrystal Investigations of Precipitates, Interfaces and Strain Fields in Ni-Ti-Nb by Various TEM Techniques. Materials Science Forum, 2013, 738-739, 65-71.	0.3	3
110	Mapping electronic reconstruction at the metal-insulator interface in LaVO <mml:math xmlns:mml="http://www.w3.org/1998/Math/MathML" display="inline"><mml:msub><mml:mrow /><mml:mn>3</mml:mn></mml:mrow </mml:msub>/SrVO<mml:math xmlns:mml="http://www.w3.org/1998/Math/MathML" display="inline"><mml:msub><mml:mrow /><mml:mn>3</mml:mn></mml:mrow </mml:msub>heterostructures. Physical Review B, 2013, 88, .</mml:math </mml:math 	3.2	16
111	Procedure to count atoms with trustworthy single-atom sensitivity. Physical Review B, 2013, 87, .	3.2	121
112	Beyond the limits of imaging: advances and applications of model-based scanning transmission electron microscopy. Microscopy and Microanalysis, 2012, 18, 356-357.	0.4	0
113	Exit wave reconstruction from focal series of HRTEM images, single crystal XRD and total energy studies on Sb _{<i>x</i>} WO _{3+<i>y</i>} (<i>x</i> â ¹ /4 0.11). Zeitschrift Fur Kristallographie - Crystalline Materials, 2012, 227, 341-349.	0.8	8
114	Atomic scale dynamics of ultrasmall germanium clusters. Nature Communications, 2012, 3, 897.	12.8	101
115	Advanced Electron Microscopy for Advanced Materials. Advanced Materials, 2012, 24, 5655-5675.	21.0	115
116	Fully Automated Measurement of the Modulation Transfer Function of Charge-Coupled Devices above the Nyquist Frequency. Microscopy and Microanalysis, 2012, 18, 336-342.	0.4	19
117	Model-based electron microscopy: From images toward precise numbers for unknown structure parameters. Micron, 2012, 43, 509-515.	2.2	20
118	Precision of three-dimensional atomic scale measurements from HRTEM images: What are the limits?. Ultramicroscopy, 2012, 114, 20-30.	1.9	12
119	Correction of non-linear thickness effects in HAADF STEM electron tomography. Ultramicroscopy, 2012, 116, 8-12.	1.9	75
120	Direct structure inversion from exit waves. Part II: A practical example. Ultramicroscopy, 2012, 116, 77-85.	1.9	15
121	Direct Observation of Ferrielectricity at Ferroelastic Domain Boundaries in CaTiO ₃ by Electron Microscopy. Advanced Materials, 2012, 24, 523-527.	21.0	225
122	High-Resolution Visualization Techniques: Structural Aspects. Springer Series in Materials Science, 2012, , 135-149.	0.6	2
123	Ultra-High Resolution Electron Tomography for Materials Science: a Roadmap. Microscopy and Microanalysis, 2011, 17, 934-935.	0.4	2
124	Three-Dimensional Atomic Imaging of Colloidal Core–Shell Nanocrystals. Nano Letters, 2011, 11, 3420-3424.	9.1	134
125	Three-dimensional atomic imaging of crystalline nanoparticles. Nature, 2011, 470, 374-377.	27.8	503
126	A method to determine the local surface profile from reconstructed exit waves. Ultramicroscopy, 2011, 111, 1352-1359.	1.9	4

8

#	Article	IF	CITATIONS
127	High precision measurements of atom column positions using model-based exit wave reconstruction. Ultramicroscopy, 2011, 111, 1475-1482.	1.9	13
128	Throughput maximization of particle radius measurements through balancing size versus current of the electron probe. Ultramicroscopy, 2011, 111, 940-947.	1.9	12
129	Optimized fabrication of high-quality La _{0.67} Sr _{0.33} MnO ₃ thin films considering all essential characteristics. Journal Physics D: Applied Physics, 2011, 44, 205001.	2.8	105
130	Computational Aspects in Quantitative EELS. Microscopy and Microanalysis, 2010, 16, 240-241.	0.4	0
131	A model based reconstruction technique for depth sectioning with scanning transmission electron microscopy. Ultramicroscopy, 2010, 110, 548-554.	1.9	20
132	Direct structure inversion from exit waves. Ultramicroscopy, 2010, 110, 527-534.	1.9	37
133	Linear versus non-linear structural information limit in high-resolution transmission electron microscopy. Ultramicroscopy, 2010, 110, 1404-1410.	1.9	8
134	Effect of amorphous layers on the interpretation of restored exit waves. Ultramicroscopy, 2009, 109, 237-246.	1.9	16
135	Quantitative atomic resolution mapping using high-angle annular dark field scanning transmission electron microscopy. Ultramicroscopy, 2009, 109, 1236-1244.	1.9	195
136	A model based atomic resolution tomographic algorithm. Ultramicroscopy, 2009, 109, 1485-1490.	1.9	20
137	Atomic Resolution Mapping Using Quantitative High-angle Annular Dark Field Scanning Transmission Electron Microscopy. Microscopy and Microanalysis, 2009, 15, 464-465.	0.4	1
138	Argand plot: a sensitive fingerprint for electron channelling. , 2008, , 167-168.		0
139	The benefits of statistical parameter estimation theory for quantitative interpretation of electron microscopy data. , 2008, , 97-98.		0
140	Structural, Chemical And Electronic Characterization Of Ceramic Materials Using Quantitative (Scanning) Transmission Electron Microscopy Microscopy and Microanalysis, 2007, 13, 332-333.	0.4	1
141	The Notion of Resolution. , 2007, , 1228-1265.		7
142	Electron channelling based crystallography. Ultramicroscopy, 2007, 107, 551-558.	1.9	40
143	Resolution of coherent and incoherent imaging systems reconsidered - Classical criteria and a statistical alternative. Optics Express, 2006, 14, 3830.	3.4	75
144	Electronically coupled complementary interfaces between perovskite band insulators. Nature Materials, 2006, 5, 556-560.	27.5	325

#	Article	IF	CITATIONS
145	An efficient way of including thermal diffuse scattering in simulation of scanning transmission electron microscopic images. Ultramicroscopy, 2006, 106, 933-940.	1.9	23
146	Model-based quantification of EELS spectra: Including the fine structure. Ultramicroscopy, 2006, 106, 976-980.	1.9	40
147	Statistical Estimation of Atomic Positions from Exit Wave Reconstruction with a Precision in the Picometer Range. Physical Review Letters, 2006, 96, 096106.	7.8	82
148	Obstacles on the Road Towards Atomic Resolution Tomography. Microscopy and Microanalysis, 2005, 11, .	0.4	0
149	Maximum likelihood estimation of structure parameters from high resolution electron microscopy images. Part I: A theoretical framework. Ultramicroscopy, 2005, 104, 83-106.	1.9	98
150	Maximum likelihood estimation of structure parameters from high resolution electron microscopy images. Part II: A practical example. Ultramicroscopy, 2005, 104, 107-125.	1.9	62
151	Model based quantification of EELS spectra. Ultramicroscopy, 2004, 101, 207-224.	1.9	174
152	How to optimize the experimental design of quantitative atomic resolution TEM experiments?. Micron, 2004, 35, 425-429.	2.2	23
153	Physical Limits on Atomic Resolution. Microscopy and Microanalysis, 2004, 10, 153-157.	0.4	9
154	Statistical Experimental Design for Quantitative Atomic Resolution Transmission Electron Microscopy. Advances in Imaging and Electron Physics, 2004, 130, 1-164.	0.2	17
155	Is atomic resolution transmission electron microscopy able to resolve and refine amorphous structures?. Ultramicroscopy, 2003, 98, 27-42.	1.9	40
156	Unconventional Specimen Preparation Techniques Using High Resolution Low Voltage Field Emission Scanning Electron Microscopy to Study Cell Motility, Host Cell Invasion, and Internal Cell Structures in Toxoplasma gondii. Microscopy and Microanalysis, 2002, 8, 94-103.	0.4	12
157	High-resolution electron microscopy and electron tomography: resolution versus precision. Journal of Structural Biology, 2002, 138, 21-33.	2.8	54
158	How to Select the Items for the Shopping List of Future High Resolution Electron Microscopists?. Microscopy and Microanalysis, 2002, 8, 94-95.	0.4	11
159	High-resolution electron microscopy: from imaging toward measuring. IEEE Transactions on Instrumentation and Measurement, 2002, 51, 611-615.	4.7	20
160	Optimal experimental design of STEM measurement of atom column positions. Ultramicroscopy, 2002, 90, 273-289.	1.9	51
161	Do smaller probes in a scanning transmission electron microscope result in more precise measurement of the distances between atom columns?. The Philosophical Magazine: Physics of Condensed Matter B, Statistical Mechanics, Electronic, Optical and Magnetic Properties, 2001, 81, 1833-1846.	0.6	9
162	Does a monochromator improve the precision in quantitative HRTEM?. Ultramicroscopy, 2001, 89, 275-290.	1.9	32

#	Article	IF	CITATIONS
163	Do smaller probes in a scanning transmission electron microscope result in more precise measurement of the distances between atom columns?. The Philosophical Magazine: Physics of Condensed Matter B, Statistical Mechanics, Electronic, Optical and Magnetic Properties, 2001, 81, 1833-1846.	0.6	11

164 High resolution electron microscopy from imaging towards measuring. , 0, , .